

# Structure and Luminosity of Neutrino-cooled Accretion Disks

Tong Liu, Wei-Min Gu, Li Xue, and Ju-Fu Lu\*

*Department of Physics and Institute of Theoretical Physics and Astrophysics,  
Xiamen University, Xiamen, Fujian 361005, China*

\*lujf@xmu.edu.cn

## ABSTRACT

Neutrino-cooled hyperaccretion disks around stellar mass black holes are plausible candidates for the central engine of gamma-ray bursts. We calculate the one-dimensional structure and the annihilation luminosity of such disks. The neutrino optical depth is of crucial importance in determining the neutrino cooling rate and is in turn dependent on the electron fraction, the free nucleon fraction, and the electron degeneracy, with given density and temperature of the disk matter. We construct a bridging formula for the electron fraction that works for various neutrino optical depths, and give exact definitions for the free proton fraction and free neutron fraction. We show that the electron degeneracy has important effects in the sense that it enlarges the absorption optical depth for neutrinos, and it along with the neutronization processes favored by high temperature cause the electron fraction to drop to be below 0.1 in the inner region of the disk. The resulting neutrino annihilation luminosity is considerably reduced comparing with that obtained in previous works where the electron degeneracy was not considered and the electron fraction was simply taken to be 0.5, but it is still likely to be adequate for gamma-ray bursts, and it is ejected mainly from the inner region of the disk and has an anisotropic distribution.

*Subject headings:* accretion, accretion disks - black hole physics - gamma rays: bursts - neutrinos

## 1. Introduction

Theoretical models for gamma-ray bursts (GRBs) can be divided into two categories: those named fireball models that treat the shock interaction of relativistic outflows and production of gamma rays and afterglows in other wavelengths (see, e.g., Mészáros 2002 and Zhang & Mészáros 2004 for reviews), and those that explore the central engine of the fireball,

i.e., the energy source of relativistic outflows. Most popular models in the latter category are in common invoking a stellar-mass black hole accreting with a hypercritical rate, of the order of  $1 M_{\odot} \text{ s}^{-1}$ . The main problem in these models is how to convert some fraction of the released gravitational energy of the accreted matter into a relativistic outflow, creating an explosion with energy  $\sim 10^{50}$ - $10^{52}$  ergs (depending on whether emission is isotropic or it is beamed). Two mechanisms have been proposed to tackle this problem: the neutrino emission and annihilation, and the energy extraction from the accretion disk and/or the black hole via magnetohydrodynamical processes (see, e.g., Popham et al. 1999 and Di Matteo et al. 2002 for references). The former mechanism is easier to understand and can be calculated more accurately, and is the topic we wish to discuss in this paper.

In the inner region of such a hyperaccretion disk the density and temperature are so high ( $\rho \sim 10^{10} \text{ g cm}^{-3}$ ,  $T \sim 10^{10} \text{ K}$ ) that photons are totally trapped, and large amounts of energetic neutrinos are emitted, carrying away the viscous dissipation energy of accreted gas. Annihilation of some fraction of emitted neutrinos produces a relativistic electron-positron outflow to power a GRB. The properties of such a neutrino-cooled accretion disk model were first worked out in details by Popham et al. (1999). From the observational point of view, the key question to be answered in this model is whether the neutrino annihilation can indeed provide sufficient energy for GRBs. Popham et al. (1999) gave a positive answer to this question, but they assumed a priori that the accretion disk is transparent for neutrinos, thus their neutrino radiation luminosity (before annihilation)  $L_{\nu}$  and accordingly neutrino annihilation luminosity  $L_{\nu\bar{\nu}}$  might be overestimated. Later, Di Matteo et al. (2002) recalculated  $L_{\nu}$  and  $L_{\nu\bar{\nu}}$  in the neutrino-cooled accretion disk model, taking the neutrino opacity into account. They obtained that even for a modest mass accretion rate the inner region of the disk becomes opaque and neutrinos are sufficiently trapped, the resulting  $L_{\nu\bar{\nu}}$  is  $\lesssim 10^{50} \text{ ergs s}^{-1}$  and is inadequate for GRBs. In a recent work (Gu et al. 2006) we showed that when the general relativistic effect is considered and the contribution from the optically thick region is included, the neutrino-cooled accretion disk can work as the central engine for GRBs, although the correct  $L_{\nu\bar{\nu}}$  is somewhat lower than that of Popham et al. (1999) because of the effect of neutrino opacity.

In addition to the general relativity and the neutrino opacity, there are certainly other factors that may influence the neutrino radiation and annihilation of a neutrino-cooled accretion disk, such as the electron degeneracy and the electron fraction. In our previous work (Gu et al. 2006) the treatment of electron degeneracy was oversimplified, and the electron fraction  $Y_e$  was simply taken to be 0.5, i.e., assuming an equal mix of protons and neutrons since  $Y_e = n_p / (n_p + n_n)$ , where  $n_p$  and  $n_n$  are the total number density of protons and that of neutrons, respectively. Kohri & Mineshige (2002) pointed out that when electrons are degenerate, there emerges an important consequence that the electron-positron pair creation

and accordingly the neutrino emission are suppressed. Kohri et al. (2005) took great care to calculate the ratio of free neutrons to free protons  $\tilde{n}_n/\tilde{n}_p$  since this ratio has a large effect on the neutrino emission rates: the true ratio  $\tilde{n}_n/\tilde{n}_p > 1$  (or  $Y_e < 0.5$ ) resulted from neutronization processes will also lead to a suppression of neutrino emission (note that they did not distinguish between  $n_n$ ,  $n_p$  and  $\tilde{n}_n, \tilde{n}_p$ , see §2.3.1). They made calculations for the neutrino emission rates and other quantities even in the delicate regime where the electron degeneracy is moderate, which is also a significant improvement over previous works. Lee et al. (2005) also considered the effects of electron degeneracy and electron fraction in neutrino-cooled accretion disks: they used an expression for the pressure of ultra-relativistic electrons with arbitrary degeneracy and calculated  $Y_e$  with an approximate bridging formula that allows for a transition from the neutrino optically thin to optically thick regime. These works (Kohri & Mineshige 2002; Kohri et al. 2005; Lee et al. 2005) made advances in microphysics, but they were within the Newtonian framework. Very recently, Chen & Beloborodov (2006) presented fully relativistic calculations of the structure of neutrino-cooled accretion disks around Kerr black holes and proved that both the electron degeneracy and the electron fraction dramatically affect the disk and its neutrino emission.

It is seen from the above brief review that the electron degeneracy and the lower electron fraction certainly suppress the neutrino emission and reduce the neutrino annihilation luminosity of a neutrino-cooled accretion disk. The question remains whether the reduced neutrino annihilation luminosity is still adequate for GRBs. In this paper we try to refine our previous results of the structure and luminosity of neutrino-cooled accretion disks by considering the relevant microphysics more completely and more accurately.

## 2. Physics of Neutrino-cooled Accretion Disks

### 2.1. Hydrodynamics

We limit the central accreting black hole to be a non-rotating one, its general relativistic effect is simulated by the well-known Paczyński & Wiita (1980) potential  $\Phi = -GM/(R - R_g)$ , where  $M$  is the black hole mass,  $R$  is the radius, and  $R_g = 2GM/c^2$  is the Schwarzschild radius.

As in the relevant previous works, the hydrodynamics of hyperaccretion disks is expected to be similar to that of normal accretion disks in X-ray binaries, and is well approximated by that of steady axisymmetric height-averaged accretion flows (e.g., Chap. 3 of Kato et al. 1998). Accretion in the disk is driven by viscous stress, and the kinematic viscosity coefficient is expressed as  $\nu = \alpha_c H$ , where  $H$  is the half thickness of the disk;  $c_s = (P/\rho)^{1/2}$  is the

isothermal sound speed, with  $P$  and  $\rho$  being the pressure and mass density, respectively; and  $\alpha$  is a dimensionless constant parameter that absorbs all the detailed microphysics of viscous processes. The angular velocity is approximately Keplerian, i.e.,  $\Omega = \Omega_K = (GM/R)^{1/2}/(R - R_g)$ . The disk is in the vertical hydrostatic equilibrium, and this gives  $H = c_s/\Omega_K$ . With these simplifications the problem is reduced to be one-dimensional, i.e., all physical quantities depend on  $R$  only.

The constant mass accretion rate  $\dot{M}$  is expressed from the continuity equation as

$$\dot{M} = -4\pi R H \rho v, \quad (1)$$

where  $v$  is the radial velocity that can be read from the angular momentum equation as

$$v = \alpha H c_s (1 - j/\Omega_K R^2)^{-1} \frac{d \ln \Omega_K}{dR}, \quad (2)$$

where  $j$  is an integration constant determined by the zero-torque boundary condition at the last stable orbit, and it represents the specific angular momentum (per unit mass) of the matter accreted into the black hole.

## 2.2. Thermodynamics

The energy equation is generally written as the balance between the viscous heating and the cooling rates (per unit area of a half-disk above or below the equator),

$$Q_{\text{vis}} = Q^-. \quad (3)$$

The viscous heating rate  $Q_{\text{vis}}$  is similar to that of normal accretion disks,

$$Q_{\text{vis}} = -\frac{1}{4\pi} \dot{M} \Omega_K R (1 - j/\Omega_K R^2) \frac{d\Omega_K}{dR}. \quad (4)$$

But the cooling rate  $Q^-$  is crucially different, it has three contributions:

$$Q^- = Q_{\text{photodis}} + Q_{\text{adv}} + Q_{\nu}. \quad (5)$$

In this equation there is no cooling term of photon radiation (it is practically zero in our calculations). Instead, photons are totally trapped in the disk, so they contribute to the advective cooling and the pressure (see below). The cooling rate by photodisintegration of  $\alpha$ -particles  $Q_{\text{photodis}}$  is

$$Q_{\text{photodis}} = 6.8 \times 10^{28} \rho_{10} v H \frac{dX_{\text{nuc}}}{dR} \text{ cgs units}, \quad (6)$$

where  $\rho_{10} \equiv \rho/10^{10} \text{ g cm}^{-3}$ , and  $X_{\text{nuc}}$  is the mass fraction of free nucleons (e.g., Kohri et al. 2005). The advective cooling rate  $Q_{\text{adv}}$  is

$$Q_{\text{adv}} = \rho v H T \frac{ds}{dR} \approx -\xi v \frac{H}{R} T \left( \frac{4}{3} a T^3 + \frac{3 k_B \rho}{2 m_u} \frac{1 + 3X_{\text{nuc}}}{4} + \frac{4 u_\nu}{3 T} \right), \quad (7)$$

where  $s$  is the specific entropy,  $\xi \propto -d \ln s / d \ln R$  is taken to be equal to 1, i.e.,  $ds/dR$  is approximated as  $s/R$  (Kohri & Mineshige 2002), and  $m_u$  is the mean mass of a nucleon. The entropy of degenerate particles is small and can be neglected. The three terms in the brackets of equation (7) are the entropy density of photons, of free nucleons and  $\alpha$ -particles, and of neutrinos, respectively; and  $u_\nu$  is the energy density of neutrinos, for which we adopt a bridging formula valid in both the optically thin and thick regimes (Popham & Narayan 1995; Di Matteo et al. 2002),

$$u_\nu = \sum_i \frac{(7/8) a T^4 (\tau_{\nu_i}/2 + 1/\sqrt{3})}{\tau_{\nu_i}/2 + 1/\sqrt{3} + 1/(3\tau_{a,\nu_i})}, \quad (8)$$

where  $\tau_{\nu_i}$  is the total optical depth for neutrinos,  $\tau_{a,\nu_i}$  is the absorption optical depth for neutrinos, and the subscript  $i$  runs for the three species of neutrinos  $\nu_e$ ,  $\nu_\mu$ , and  $\nu_\tau$ . The cooling rate due to neutrino loss  $Q_\nu$  is expressed in accordance with the above equation (Kohri et al. 2005),

$$Q_\nu = \sum_i \frac{(7/8) \sigma T^4}{(3/4) [\tau_{\nu_i}/2 + 1/\sqrt{3} + 1/(3\tau_{a,\nu_i})]}. \quad (9)$$

The equation of state is also very different from that of normal accretion disks, as the contributions to the pressure from degenerate electrons (we assume that nucleons are not degenerate throughout the present paper) and from neutrinos should be included, it is written as

$$P = P_{\text{gas}} + P_{\text{rad}} + P_e + P_\nu. \quad (10)$$

The gas pressure from free nucleons and  $\alpha$ -particles  $P_{\text{gas}}$  is

$$P_{\text{gas}} = \frac{k_B \rho T}{m_u} \frac{1 + 3X_{\text{nuc}}}{4}. \quad (11)$$

The photon radiation pressure  $P_{\text{rad}}$  is

$$P_{\text{rad}} = a T^4 / 3. \quad (12)$$

The electron pressure  $P_e$  is from both electrons and positrons and should be calculated using the exact Fermi-Dirac distribution. No asymptotic expansions are valid because at

different radii electrons may be with different degrees of degeneracy and may be relativistic or nonrelativistic. It reads

$$P_e = P_{e^-} + P_{e^+}, \quad (13)$$

with

$$P_{e^\mp} = \frac{1}{3\pi^2\hbar^3c^3} \int_0^\infty dp \frac{p^4}{\sqrt{p^2c^2 + m_e^2c^4}} \frac{1}{e^{(\sqrt{p^2c^2 + m_e^2c^4} \mp \mu_e)/k_B T} + 1}, \quad (14)$$

where  $\mu_e$  is the chemical potential of electrons, and the electron degeneracy is measured by the degeneracy parameter defined as  $\eta_e = \mu_e/k_B T$ . We agree with Lee et al. (2005) that since the presence of relativistic  $e^-e^+$  pairs is automatically taken into account in the expression for  $P_e$ , there is no alteration to the numerical factor 1/3 in the expression for  $P_{\text{rad}}$ , nor to the factor 4/3 for the photon entropy in equation (7). The neutrino pressure  $P_\nu$  is

$$P_\nu = u_\nu/3. \quad (15)$$

### 2.3. Microphysics

All the equations in the above two subsections can be combined into only two equations, i.e., equations (1) and (3). In these two equations there are seven unknown quantities, namely  $\rho$ ,  $T$ ,  $X_{\text{nuc}}$ ,  $\tau_{\nu_i}$  ( $\nu_i = \nu_e, \nu_\mu, \nu_\tau$ ), and  $\mu_e$  (or  $\eta_e$ ). Therefore, one has to find more equations relating these unknowns with the knowledge of microphysics.

#### 2.3.1. Neutrino optical depth

The total optical depth for neutrinos is

$$\tau_{\nu_i} = \tau_{s,\nu_i} + \tau_{a,\nu_i}. \quad (16)$$

The optical depth for neutrinos through scattering off free nucleons,  $\alpha$ -particles, and electrons  $\tau_{s,\nu_i}$  is given by

$$\tau_{s,\nu_i} = H/\lambda_{\nu_i} = H[\sigma_{p,\nu_i}\tilde{n}_p + \sigma_{n,\nu_i}\tilde{n}_n + \sigma_{\alpha,\nu_i}n_\alpha + \sigma_{e,\nu_i}(n_{e^-} + n_{e^+})], \quad (17)$$

where  $\lambda_{\nu_i}$  is the mean free path;  $\sigma_{p,\nu_i}$ ,  $\sigma_{n,\nu_i}$ ,  $\sigma_{\alpha,\nu_i}$  and  $\sigma_{e,\nu_i}$  are the cross sections of scattering on protons, neutrons,  $\alpha$ -particles, and electrons;  $\tilde{n}_p$ ,  $\tilde{n}_n$ ,  $n_\alpha$ ,  $n_{e^-}$  and  $n_{e^+}$  are the number

densities of free protons, free neutrons,  $\alpha$ -particles, electrons, and positrons, respectively. The four cross sections are given by (Burrows & Thompson 2002)

$$\sigma_{p,\nu_i} = \frac{\sigma_0 E_{\nu_i}^2}{4} [(C_{V,\nu_i} - 1)^2 + 3g_A^2 (C_{A,\nu_i} - 1)^2], \quad (18)$$

$$\sigma_{n,\nu_i} = \frac{\sigma_0 E_{\nu_i}^2}{4} \frac{1 + 3g_A^2}{4}, \quad (19)$$

$$\sigma_{\alpha,\nu_i} = 4\sigma_0 E_{\nu_i}^2 \sin^4 \theta_W, \quad (20)$$

$$\sigma_{e,\nu_i} = \frac{3k_B T \sigma_0 E_{\nu_i}}{8m_e c^2} \left(1 + \frac{\eta_e}{4}\right) [(C_{V,\nu_i} + C_{A,\nu_i})^2 + \frac{1}{3}(C_{V,\nu_i} - C_{A,\nu_i})^2], \quad (21)$$

where  $\sigma_0 = 1.76 \times 10^{-44} \text{cm}^2$ ,  $E_{\nu_i}$  is the mean energy of neutrinos in units of  $(m_e c^2)$ ,  $g_A \approx 1.26$ ,  $\sin^2 \theta_W \approx 0.23$ ,  $C_{V,\nu_e} = 1/2 + 2 \sin^2 \theta_W$ ,  $C_{V,\nu_\mu} = C_{V,\nu_\tau} = -1/2 + 2 \sin^2 \theta_W$ ,  $C_{A,\nu_e} = C_{A,\bar{\nu}_\mu} = C_{A,\bar{\nu}_\tau} = 1/2$ ,  $C_{A,\nu_e} = C_{A,\nu_\mu} = C_{A,\nu_\tau} = -1/2$ . Since  $\tilde{n}_p = n_p - 2n_\alpha$  and  $\tilde{n}_n = n_n - 2n_\alpha$ , the free proton fraction  $Y_p$ , the free neutron fraction  $Y_n$ , and the  $\alpha$ -particle fraction  $Y_\alpha$  are related to  $Y_e$  and  $X_{\text{nuc}}$  as

$$Y_p = \frac{\tilde{n}_p}{n_p + n_n} = Y_e - \frac{1 - X_{\text{nuc}}}{2}, \quad (22)$$

$$Y_n = \frac{\tilde{n}_n}{n_p + n_n} = 1 - Y_e - \frac{1 - X_{\text{nuc}}}{2}, \quad (23)$$

$$Y_\alpha = \frac{n_\alpha}{n_p + n_n} = \frac{1 - X_{\text{nuc}}}{4}, \quad (24)$$

and  $n_{e^-}$ ,  $n_{e^+}$  are given by the Fermi-Dirac integration,

$$n_{e^\mp} = \frac{1}{\hbar^3 \pi^2} \int_0^\infty dp p^2 \frac{1}{e^{(\sqrt{p^2 c^2 + m_e^2 c^4} \mp \mu_e)/k_B T} + 1} \quad (25)$$

(cf. Kohri et al. 2005, they took  $\tilde{n}_p = n_p$  and  $\tilde{n}_n = n_n$ , and thus  $Y_p = Y_e$  and  $Y_n = 1 - Y_e$ , which are valid only for the completely dissociated matter, i.e.,  $X_{\text{nuc}} = 1$ ).

The absorption depth for neutrinos  $\tau_{a,\nu_i}$  is defined by

$$\tau_{a,\nu_i} = \frac{q_{\nu_i} H}{4(7/8)\sigma T^4}, \quad (26)$$

where  $q_{\nu_i}$  is the total neutrino cooling rate (per unit volume) and is the sum of four terms,

$$q_{\nu_i} = q_{\text{URCA}} + q_{e^-e^+} + q_{\text{brem}} + q_{\text{plasmon}}. \quad (27)$$

The neutrino cooling rate due to the URCA processes  $q_{\text{URCA}}$  relates only to  $\nu_e$  and is represented by the sum of three terms (Chap. 11 of Shapiro & Teukolsky 1983; Yuan 2005),

$$q_{\text{URCA}} = q_{p+e^- \rightarrow n+\nu_e} + q_{n+e^+ \rightarrow p+\bar{\nu}_e} + q_{n \rightarrow p+e^-+\bar{\nu}_e}, \quad (28)$$

with

$$q_{p+e^- \rightarrow n+\nu_e} = \frac{G_F^2 \cos^2 \theta_c}{2\pi^2 \hbar^3 c^2} (1 + 3g_A^2) \tilde{n}_p \int_Q^\infty dE_e E_e \sqrt{E_e^2 - m_e^2 c^4} (E_e - Q)^3 f_{e^-}, \quad (29)$$

$$q_{n+e^+ \rightarrow p+\bar{\nu}_e} = \frac{G_F^2 \cos^2 \theta_c}{2\pi^2 \hbar^3 c^2} (1 + 3g_A^2) \tilde{n}_n \int_{m_e c^2}^\infty dE_e E_e \sqrt{E_e^2 - m_e^2 c^4} (E_e + Q)^3 f_{e^+}, \quad (30)$$

$$q_{n \rightarrow p+e^-+\bar{\nu}_e} = \frac{G_F^2 \cos^2 \theta_c}{2\pi^2 \hbar^3 c^2} (1 + 3g_A^2) \tilde{n}_n \int_{m_e c^2}^Q dE_e E_e \sqrt{E_e^2 - m_e^2 c^4} (Q - E_e)^3 (1 - f_{e^-}), \quad (31)$$

where  $G_F \approx 1.436 \times 10^{-49}$  ergs cm<sup>3</sup>,  $\cos^2 \theta_c \approx 0.947$ ,  $Q = (m_n - m_p)c^2$ , and  $f_{e^\mp} = \{\exp[(E_e \mp \mu_e)/k_B T] + 1\}^{-1}$  is the Fermi-Dirac function. The last term in the right hand side of equation (28), i.e., equation (31), is small comparing with the other two terms, and was usually not included in the literature. The electron-positron pair annihilation rate into neutrinos  $q_{e^-e^+}$  is (e.g., Itoh et al. 1989)

$$q_{e^-e^+ \rightarrow \nu_e \bar{\nu}_e} \approx 3.4 \times 10^{33} T_{11}^9 \text{ ergs cm}^{-3} \text{ s}^{-1}, \quad (32)$$

$$q_{e^-e^+ \rightarrow \nu_\mu \bar{\nu}_\mu} = q_{e^-e^+ \rightarrow \nu_\tau \bar{\nu}_\tau} \approx 0.7 \times 10^{33} T_{11}^9 \text{ ergs cm}^{-3} \text{ s}^{-1}, \quad (33)$$

where  $T_{11} \equiv T/10^{11}$  K. Expressions (32) and (33) are valid in the nondegenerate limit  $\eta_e \ll 1$ , and when electrons are degenerate  $q_{e^-e^+}$  becomes negligible. The nucleon-nucleon bremsstrahlung rate  $q_{\text{brem}}$  through the processes  $n + n \rightarrow n + n + \nu_i + \bar{\nu}_i$  is the same for the three species of neutrinos (Hannestad & Raffelt 1998; Burrows et al. 2000),

$$q_{\text{brem}} \approx 1.5 \times 10^{27} \rho_{10}^2 T_{11}^{5.5} \text{ ergs cm}^{-3} \text{ s}^{-1}. \quad (34)$$

As to the plasmon decay rate  $q_{\text{plasmon}}$ , only that through the process  $\tilde{\gamma} \rightarrow \nu_e + \bar{\nu}_e$  needs to be considered, where plasmons  $\tilde{\gamma}$  are photons interacting with electrons,

$$q_{\text{plasmon}} \approx 1.5 \times 10^{32} T_{11}^9 \gamma_p^6 \exp(-\gamma_p) (1 + \gamma_p) \left(2 + \frac{\gamma_p^2}{1 + \gamma_p}\right) \text{ ergs cm}^{-3} \text{ s}^{-1}, \quad (35)$$

where  $\gamma_p = 5.565 \times 10^{-2} [(\pi^2 + 3\eta_e^2)/3]^{1/2}$  (Ruffert et al. 1996). It is expected that  $q_{\text{brem}}$  and  $q_{\text{plasmon}}$  can become important only at very high electron degeneracy.

### 2.3.2. Electron Fraction

It is seen that the electron fraction  $Y_e$  mentioned in Introduction has appeared in the expression of neutrino optical depth  $\tau_{\nu_i}$ . In order to calculate  $\tau_{\nu_i}$  and accordingly the neutrino cooling rate  $Q_\nu$  (see eq. [9]), more knowledge about  $Y_e$  is required.

Beloborodov (2003) proved that  $\beta$ -equilibrium among free neutrons, free protons, and electrons is established in disks with  $\dot{M} \gtrsim 10^{31} (\alpha/0.1)^{9/5} (M/M_\odot)^{6/5} \text{ g s}^{-1}$ , a condition that is likely to be fulfilled for hyperaccretion disks; and noted that a distinction needs to be made to determine the equilibrium composition depending on the optical depth of the disk material. Kohri et al. (2005) discussed various timescales in neutrino-cooled accretion disks in details, and showed that for sufficiently large  $\dot{M}$  and not too large  $R$  the timescale for the reactions from proton to neutron and from neutron to proton is shorter than the dynamical timescale (the accretion time), i.e., the  $\beta$ -equilibrium is likely to be realized.

If the disk material is opaque to neutrinos, there are reversible reactions  $e^- + p \rightleftharpoons n + \nu_e$  and  $e^+ + n \rightleftharpoons p + \bar{\nu}_e$ . The chemical potential of neutrinos can be ignored because the number density of neutrinos and that of antineutrinos are likely to be equal, then the  $\beta$ -equilibrium condition is

$$\mu_n = \mu_p + \mu_e, \quad (36)$$

where  $\mu_n$  and  $\mu_p$  are chemical potentials of neutrons and protons, respectively. On the other hand, if the material is transparent to neutrinos, there are no reversible reactions as for the neutrino opaque material, but the  $\beta$ -equilibrium can be reached when the rate of reaction  $e^- + p \rightarrow n + \nu_e$  is equal to that of reaction  $e^+ + n \rightarrow p + \bar{\nu}_e$ . Yuan (2005) calculated these two rates and obtained

$$\mu_n = \mu_p + 2\mu_e. \quad (37)$$

The neutron-to-proton ratio in  $\beta$ -equilibrium is given by

$$\frac{\tilde{n}_n}{\tilde{n}_p} = \exp [(\mu_n - \mu_p - Q)/k_B T], \quad (38)$$

which results in

$$\lg \frac{\tilde{n}_n}{\tilde{n}_p} = \frac{\mu_e - Q}{k_B T}, \quad (39)$$

for the neutrino opaque limit, and

$$\lg \frac{\tilde{n}_n}{\tilde{n}_p} = \frac{2\mu_e - Q}{k_B T}, \quad (40)$$

for the neutrino transparent limit. In order to allow for a transition from the optically thin to optically thick regime, we adopt a treatment similar to that in Lee et al. (2005), i.e. introducing a weight factor  $f(\tau_\nu) = \exp(-\tau_\nu)$  and writing in a combined form,

$$\lg \frac{\tilde{n}_n}{\tilde{n}_p} = f(\tau_\nu) \frac{2\mu_e - Q}{k_B T} + [1 - f(\tau_\nu)] \frac{\mu_e - Q}{k_B T}. \quad (41)$$

By using the relation  $Y_e = n_p/(n_p + n_n)$  and equations (22), (23), and (24) we finally arrive at

$$Y_e = \frac{1}{2}(1 - X_{\text{nuc}}) + \frac{X_{\text{nuc}}}{1 + \exp\left\{\frac{[1+f(\tau_\nu)]\mu_e - Q}{k_B T}\right\}}. \quad (42)$$

Some comments on equation (42) are in order. First, this equation is more exact than equation (12) of Lee et al. (2005), theirs is the first term of the expansion of ours. Second, we notice that Kohri et al. (2005) discussed the ratio  $\tilde{n}_n/\tilde{n}_p$  at length. They started with considering the transition rates from proton to neutron and from neutron to proton, then obtained the expression of  $\tilde{n}_n/\tilde{n}_p$ , i.e., equation (39) for the neutrino opaque limit, and adopted an approximate procedure to estimate this ratio for the neutrino optically thin regime. We stress that equation (40) is rigorous for the neutrino transparent limit, since it is also derived from the transition rates between protons and neutrons (Yuan 2005); then we construct equation (42) as a bridging formula between the opaque and transparent limits and expect it to work for the regime where the neutrino optical depth is moderate.

An additional relation between  $Y_e$  and  $X_{\text{nuc}}$  can be found from the equation of nuclear statistical equilibrium (e.g., Meyer 1994),

$$Y(Z, A) = G(Z, A) [\zeta(3)^{A-1} \pi^{(1-A)/2} 2^{(3A-5)/2}] A^{3/2} \left(\frac{k_B T}{m_u c^2}\right)^{3(A-1)/2} \phi^{1-A} Y_p^Z Y_n^{A-Z} \exp\left[\frac{B(Z, A)}{k_B T}\right], \quad (43)$$

where  $Y(Z, A)$  is the mass fraction of a kind of particles with the charge number  $Z$  and mass number  $A$ ,  $G(Z, A)$  is the nuclear partition function,  $\zeta(3)$  is the Riemann zeta function of argument 3,  $\phi = [2\zeta(3)(k_B T)^3]/[\pi^2(\hbar c)^3 \rho N_A]$  is the photon-to-baryon ratio,  $N_A$  is the Avagadro constant, and  $B(Z, A)$  is the binding energy of the nucleus. As in all the

previous works, we assume that all heavy nuclei are  $\alpha$ -particles. This should be a reasonable assumption because all nuclei heavier than  $\alpha$ -particles contain approximately equal numbers of neutrons and protons. Then by using equations (22), (23), and (24), equation (43) yields

$$4\left(Y_e - \frac{1 - X_{\text{nuc}}}{2}\right)\left(1 - Y_e - \frac{1 - X_{\text{nuc}}}{2}\right)(1 - X_{\text{nuc}})^{-1/2} = 8.71 \times 10^4 \rho_{10}^{-3/2} T_{11}^{9/4} \exp(-1.64/T_{11}). \quad (44)$$

Only Chen & Beloborodov (2006) adopted this equation, while other previous works used a simple expression of  $X_{\text{nuc}}$  that was obtained by taking  $Y_e = 0.5$  and did not reflect the interdependence between  $Y_e$  and  $X_{\text{nuc}}$  (e.g., eq. [40] of Kohri et al. 2005).

### 2.3.3. Electron Chemical Potential

The electron chemical potential is determined by the condition of charge neutrality among protons, electrons, and positrons,

$$n_p = \frac{\rho Y_e}{m_u} = n_{e^-} - n_{e^+}, \quad (45)$$

with  $n_{e^-}$  and  $n_{e^+}$  given in equation (25).

## 2.4. Summary of Equations

The system of equations is closed, as there are eight equations, i.e., equations (1), (3), (42), (44), (45), and three equations (16) for eight independent unknowns  $\rho, T, \tau_{\nu_e}, \tau_{\nu_\mu}, \tau_{\nu_\tau}, X_{\text{nuc}}, Y_e,$  and  $\mu_e$  (or  $\eta_e$ ), which can be numerically solved as functions of  $R$  with given constant parameters  $M, \dot{M}, \alpha,$  and  $j$ . All the other quantities such as  $P$  and its components,  $Q^-$  and its components, and composition fractions  $Y_p, Y_n,$  and  $Y_\alpha$  are obtained accordingly.

Our equation set has the following advantages: (1) Effects of relevant factors are taken into account in a combined way, including the general relativity, the inner boundary condition of the disk, various processes that contribute to the neutrino cooling and the neutrino opacity, the electron degeneracy, the electron fraction, and the coexistence of electrons, positrons, free protons, free neutrons, and  $\alpha$ -particles. (2) Whenever the electron degeneracy is concerned we use the exact Fermi-Dirac integration rather than the analytical approximations that are valid only for extreme cases. (3) We take great care to calculate the neutrino optical depth and the electron fraction. In doing so, we make a careful distinction between the total nucleon number densities  $n_n, n_p$  and the free nucleon number densities  $\tilde{n}_n, \tilde{n}_p$ , so that the composition of the disk matter can be exactly described by fractions  $Y_e, Y_p, Y_n,$  and  $Y_\alpha$  ;

we propose a new bridging formula for  $Y_e$  (eq. [42]) from the  $\beta$ -equilibrium condition, which is applicable to both the neutrino optically thin and optically thick regimes; and we adopt equation (44) that connects  $Y_e$  with  $X_{\text{nuc}}$ .

### 3. Numerical Results for The Disk Structure

This section presents our results for the structure of a neutrino-cooled accretion disk, obtained by numerically solving the set of eight equations in §2. Figures 1 - 6 show physical quantities of the disk matter as functions of  $R$ . In all these figures the necessary constant parameters are fixed to be their most typical values, i.e.,  $M = 3M_\odot$ ,  $\dot{M} = 1 M_\odot \text{ s}^{-1}$  (except for Fig. 5 where  $\dot{M} = 5M_\odot \text{ s}^{-1}$ ),  $\alpha = 0.1$ , and  $j = 1.8cR_g$  (see, e.g., Gu et al. 2006 for the discussion of  $j$ ).

Figure 1 is for the density  $\rho$ , temperature  $T$ , and electron degeneracy parameter  $\eta_e$ . It is seen that from  $R = 500R_g$  inward to  $R = 3R_g$ ,  $\rho$  increases by about four orders of magnitudes (Fig. 1a),  $T$  increases by about eight times (Fig. 1b); and in the innermost region of the disk  $\rho$  reaches to  $\sim 10^{11} \text{ g cm}^{-3}$ , and  $T$  reaches to  $\sim 3 - 4 \times 10^{10} \text{ K}$ . With such densities and temperatures,  $\eta_e$  increases first with decreasing  $R$ , reaches to its maximum value at  $R \sim 65R_g$ , and then decreases with decreasing  $R$  because of increasing temperature (Fig. 1c). The behavior of  $\eta_e$  obtained by us is consistent with that of Kohri et al. (2005, Fig. 4 there); but is not so with that of Chen & Beloborodov (2006, Fig. 3 there), who got that  $\eta_e$  always increases with decreasing  $R$  in the very inner region. We think that  $\eta_e$  ought to decrease when temperature is very high. It is important to note that the value of  $\eta_e$  is of order a few, i.e., the electron degeneracy is moderate. This justifies that the exact Fermi-Dirac distribution must be used in the calculations, and analytic approximations for either extremely degenerate electrons ( $\eta_e \gg 1$ ) or fully nondegenerate electrons ( $\eta_e \ll 1$ ) are invalid for hyperaccretion disks.

Figure 2 shows the composition of disk matter. In the outer region between  $R = 500R_g$  and  $R \sim 200R_g$ , almost all  $\alpha$ -particles are not disintegrated, so that the  $\alpha$ -particles fraction  $Y_\alpha$  keeps to be  $\sim 0.25$ , the electron fraction  $Y_e$  keeps to be  $\sim 0.5$ , and the free proton fraction  $Y_p$ , the free neutron fraction  $Y_n$ , and the free nucleon fraction  $X_{\text{nuc}}$  are all keeping  $\sim 0$ . From  $R \sim 200R_g$  inwards, the disintegration of  $\alpha$ -particles causes  $Y_\alpha$  to decrease and  $X_{\text{nuc}}$  to increase dramatically. Because of the neutronization processes favored by high temperature,  $Y_n$  greatly exceeds  $Y_p$ , and  $Y_e$  decreases accordingly. In the innermost region  $R < 10R_g$ ,  $\alpha$ -particles are almost fully disintegrated, i.e.,  $Y_\alpha \sim 0$ ,  $X_{\text{nuc}} \sim 1$ ; and the neutronization makes  $Y_n$  larger than 0.9, and  $Y_p$  and  $Y_e$  smaller than 0.1.

Contributions to the total pressure  $P$  from free nucleons and  $\alpha$ -particles  $P_{\text{gas}}$ , from degenerate electrons and positrons  $P_e$ , from photon radiation  $P_{\text{rad}}$ , and from neutrinos  $P_\nu$  are drawn in Figure 3. It is seen that  $P_e > P_{\text{gas}}$  in the outer region  $R \gtrsim 100R_g$ , and  $P_{\text{gas}}$  becomes dominant at smaller radii because both of the disintegration of  $\alpha$ -particles and the decreasing degeneracy of electrons;  $P_{\text{rad}}$  is of some importance only in the outer region, and  $P_\nu$  is small even in the innermost region  $R < 10R_g$  where the disk becomes optically thick to neutrinos.

The neutrino optical depth  $\tau_{\nu_i}$  is plotted in Figure 4. Two comparisons are made in Figure 4a. First, the optical depth for electron neutrinos  $\tau_{\nu_e}$  is several times larger than that for  $\mu$ -neutrinos  $\tau_{\nu_\mu}$  and  $\tau$ -neutrinos  $\tau_{\nu_\tau}$ , and only  $\tau_{\nu_e}$  can become larger than  $2/3$  in the innermost region  $R < 10R_g$ , therefore  $\tau_{\nu_e}$  ought to be taken as the representative of  $\tau_{\nu_i}$ . Second, the contribution to  $\tau_{\nu_e}$  from absorption  $\tau_{a,\nu_e}$  is more important than that from scattering  $\tau_{s,\nu_e}$ , this is a surprising result as the general understanding in the literature was that scattering off nucleons is a far more important opacity source than absorption (e.g., Di Matteo et al. 2002; Lee et al. 2005). We notice that in calculating the neutrino cooling rate due to the URCA processes  $q_{\text{URCA}}$  (which is dominant over other neutrino cooling rates, see Fig. 4b) those authors used an approximate formula that is valid only in the nondegeneracy limit. In fact, the electron degeneracy causes  $q_{\text{URCA}}$  to increase greatly as in our calculations. According to equation (46) of Kohri & Mineshige (2002), in the complete electron degeneracy limit  $q_{\text{URCA}}$  becomes extremely large because  $q_{\text{URCA}} \propto \eta_e^9$ ! It is indeed the case as seen from Figure 4b that the contribution to  $\tau_{a,\nu_e}$  from absorption relating to the URCA processes  $\tau_{\text{URCA}}$  is most important, the contribution from neutrino annihilation into  $e^-e^+$  pairs  $\tau_{e^-e^+}$  is of some relative importance only in the very outer region, and the contributions from nucleon-nucleon bremsstrahlung  $\tau_{\text{brem}}$  and from the inverse process of plasmon decay  $\tau_{\text{plasmon}}$  are totally negligible because the electron degeneracy is not very high. As to  $\tau_{s,\nu_e}$  (Fig. 4c), the contribution through scattering off free neutrons  $\tau_{n,\nu_e}$  is dominant over other contributions due to free protons  $\tau_{p,\nu_e}$ , electrons  $\tau_{e,\nu_e}$ , and  $\alpha$ -particles  $\tau_{\alpha,\nu_e}$  ( $\tau_{\alpha,\nu_e}$  is too small to be seen in the figure), obviously because of the richness of neutrons.

Having  $\tau_{\nu_e}$  in mind, we now check the validity of our bridging formula for  $Y_e$ , i.e., equation (42). In Figure 5,  $Y_e$  calculated using equation (42) is drawn by the solid line. Here  $\dot{M} = 5M_\odot \text{ s}^{-1}$  is taken because only at such a high accretion rate the inner region of the disk can become noticeably optically thick. For comparison, the dashed line in the figure draws  $Y_e$  in the case that the disk material is assumed to be globally opaque to neutrinos, which is calculated with (see Eq. [39])

$$Y_e = \frac{1}{2}(1 - X_{\text{nuc}}) + X_{\text{nuc}} \left[ 1 + \exp\left(\frac{\mu_e - Q}{k_B T}\right) \right]^{-1}, \quad (46)$$

and the dotted line draws  $Y_e$  if the material is globally transparent to neutrinos, obtained

with the approximate formula of Beloborodov (2003),

$$Y_e = \frac{1}{2}(1 - X_{\text{nuc}}) + X_{\text{nuc}}\left[\frac{1}{2} + 0.487\left(\frac{Q/2 - \mu_e}{k_B T}\right)\right]. \quad (47)$$

These two equations do not include the effect of varying neutrino optical depth. It is clear that our equation (42) does represent a bridge between the optically very thick and optically very thin limits, and it provides a reasonable estimate of  $Y_e$  in the intermediate regime where  $Y_e$  is overestimated by equation (46) and underestimated by equation (47).

In Figure 6 we show the ratios of various cooling rates to the viscous heating rate  $Q_{\text{vis}}$ . The photon radiation cooling is never important in hyperaccretion disks (it is practically zero when we try to calculate it). Advective cooling  $Q_{\text{adv}}$  is dominant only in the outer region of the disk  $R \gtrsim 200R_g$ , because in this region the photodisintegration of  $\alpha$ -particles has not started and the neutrino emission is weak. In the middle region  $200R_g \gtrsim R \gtrsim 50R_g$ , the  $\alpha$ -particle photodisintegration cooling  $Q_{\text{photodis}}$  dominates, corresponding to a sharp decrease of  $Y_\alpha$  and increase of  $X_{\text{nuc}}$  (see Fig. 2). In the inner region  $R \lesssim 50R_g$ , the neutrino cooling  $Q_\nu$  becomes dominant as expected.

We do not present here numerical results for the disk structure with varying values of  $\alpha$  and  $\dot{M}$ . Differences caused by changing these two parameters are only quantitative and have been discussed in, e.g., Kohri et al. (2005) and Chen & Beloborodov (2006). Briefly speaking,  $\alpha$  smaller than 0.1 will make the density higher, the electron degeneracy higher, the electron fraction lower, and the neutrino-dominated region larger; and at still larger accretion rates, advection can become dominant over neutrino cooling again in a very small region ( $R < 5R_g$  for  $\dot{M}=5M_\odot \text{ s}^{-1}$ , see Fig. 3 of Gu et al. 2006), because in that region the optical depth is very large and neutrinos are trapped in the disk.

#### 4. Neutrino Radiation and Annihilation Luminosities

Having the neutrino cooling rate  $Q_\nu$ , the neutrino radiation luminosity (before annihilation)  $L_\nu$  is obtained as

$$L_\nu = 4\pi \int_{R_{in}}^{R_{out}} Q_\nu R dR. \quad (48)$$

In our calculations the inner and outer edge of the disk are taken to be  $R_{in} = 3R_g$  and  $R_{out} = 500R_g$ , respectively.

For the calculation of the neutrino annihilation luminosity we follow the approach in Ruffert et al. (1997), Popham et al. (1999), and Rosswog et al. (2003). The disk is modeled

as a grid of cells in the equatorial plane. A cell  $k$  has its mean neutrino energy  $\varepsilon_{\nu_i}^k$ , neutrino radiation luminosity  $l_{\nu_i}^k$ , and distance to a space point above (or below) the disk  $d_k$ . The angle at which neutrinos from cell  $k$  encounter antineutrinos from another cell  $k'$  at that point is denoted as  $\theta_{kk'}$ . Then the neutrino annihilation luminosity at that point is given by the summation over all pairs of cells,

$$\begin{aligned}
 l_{\nu\bar{\nu}} = & \sum_i A_{1,i} \sum_k \frac{l_{\nu_i}^k}{d_k^2} \sum_{k'} \frac{l_{\bar{\nu}_i}^{k'}}{d_{k'}^2} (\varepsilon_{\nu_i}^k + \varepsilon_{\bar{\nu}_i}^{k'}) (1 - \cos \theta_{kk'})^2 \\
 & + \sum_i A_{2,i} \sum_k \frac{l_{\nu_i}^k}{d_k^2} \sum_{k'} \frac{l_{\bar{\nu}_i}^{k'}}{d_{k'}^2} \frac{\varepsilon_{\nu_i}^k + \varepsilon_{\bar{\nu}_i}^{k'}}{\varepsilon_{\nu_i}^k \varepsilon_{\bar{\nu}_i}^{k'}} (1 - \cos \theta_{kk'}),
 \end{aligned} \tag{49}$$

where  $A_{1,i} = (1/12\pi^2)[\sigma_0/c(m_e c^2)^2][(C_{V,\nu_i} - C_{A,\nu_i})^2 + (C_{V,\nu_i} + C_{A,\nu_i})^2]$ ,  $A_{2,i} = (1/6\pi^2)(\sigma_0/c)(2C_{V,\nu_i}^2 - C_{A,\nu_i}^2)$ , with  $C_{V,\nu_i}$  and  $C_{A,\nu_i}$  given in §2.3.1. The total neutrino annihilation luminosity is obtained by the integration over the whole space outside the black hole and the disk,

$$L_{\nu\bar{\nu}} = 4\pi \int_{R_g}^{\infty} \int_H^{\infty} l_{\nu\bar{\nu}} R dR dZ. \tag{50}$$

Figure 7 shows  $L_\nu$  (the thick dashed line) and  $L_{\nu\bar{\nu}}$  (the thick solid line) with varying  $\dot{M}$  ( $M = 3M_\odot$ ,  $\alpha = 0.1$ , and  $j = 1.8cR_g$  are kept). For comparison, these two luminosities calculated in our previous work (Gu et al. 2006), where the electron degeneracy was not correctly considered and  $Y_e$  was taken to be equal to 0.5, are also given in the figure by the thin dashed line and thin solid line, respectively. It is clear that the electron degeneracy and the lower  $Y_e$  resulted from the neutronization processes indeed suppress the neutrino emission considerably, the resulting  $L_\nu$  and  $L_{\nu\bar{\nu}}$  are reduced by a factor  $\sim 30\% - 70\%$  comparing with their overestimated values in Gu et al. (2006). Even so, the correct  $L_{\nu\bar{\nu}}$  is still well above  $10^{50}$  ergs  $s^{-1}$  provided  $\dot{M} \sim 1M_\odot s^{-1}$ , and reaches to  $\sim 10^{52}$  ergs  $s^{-1}$  when  $\dot{M} \sim 10M_\odot s^{-1}$ . Therefore, based on the energy consideration, neutrino-cooled accretion disks can work as the central engine of GRBs. Note that our calculations are for a nonrotating black hole, both Popham et al. (1999) and Chen & Beloborodov (2006) have shown that a spinning (Kerr) black hole will enhance the neutrino radiation efficiency, this only strengthens our conclusion here.

In Figure 8 the corresponding neutrino radiation efficiency  $\eta_\nu (\equiv L_\nu/\dot{M}c^2)$  and neutrino annihilation efficiency  $\eta_{\nu\bar{\nu}} (\equiv L_{\nu\bar{\nu}}/L_\nu)$  are shown by the dashed line and solid line, respectively. It is seen that  $\eta_\nu$  does not change much with varying  $\dot{M}$ ; while  $\eta_{\nu\bar{\nu}}$  increases rapidly with increasing  $\dot{M}$ , this is because at higher accretion rates more neutrinos are emitted and in turn have higher probabilities to encounter with each other.

To see the spatial distribution of neutrino annihilation luminosity, we plot in Figure 9 contours of  $(2\pi R l_{\nu\bar{\nu}})$  in units of  $(\text{erg s}^{-1} \text{ cm}^{-2})$ , i.e., the neutrino annihilation luminosity of a circle with cylindrical coordinates  $R$  and  $Z$ , for  $\dot{M} = 1M_{\odot} \text{ s}^{-1}$ . The figure has two important implications. First, it demonstrates the strong focusing of neutrino annihilation towards the central region of space. In fact, by performing the integration of equation (50) out to each radius we get that nearly 60% of the total annihilation luminosity is ejected from the region  $R < 20R_g$ . Second, it shows that the annihilation luminosity varies more rapidly along the  $Z$  coordinate than along the  $R$  coordinate, indicating that this luminosity is anisotropic and most of the annihilation energy escapes outward along the angular momentum axis of the disk.

## 5. Summary and Discussion

In this paper we wish to discuss whether the annihilation of neutrinos emitted from hyperaccretion disks can provide sufficient energy for GRBs, i.e., to estimate the neutrino annihilation luminosity  $L_{\nu\bar{\nu}}$ . To do this, we need to know the neutrino optical depth  $\tau_{\nu_i}$ , because it determines the neutrino cooling rate  $Q_{\nu}$  (eq. [9]) and the neutrino radiation luminosity  $L_{\nu}$  (eq. [48]).

To calculate contributions to  $\tau_{\nu_i}$  from various absorption and scattering processes of neutrinos (eq. [16]), we need to know the composition and physical state of disk matter, namely the fractions of electrons  $Y_e$  and free nucleons  $X_{\text{nuc}}$ , and the electron chemical potential  $\mu_e$  (or electron degeneracy  $\eta_e$ ), with given density  $\rho$  and temperature  $T$ . We give exact definitions of the free proton fraction  $Y_p$  and free neutron fraction  $Y_n$  and their relations to  $Y_e$  and  $X_{\text{nuc}}$ , and get three equations (eqs. [42], [44], and [45]) from the conditions of  $\beta$ -equilibrium, nuclear statistical equilibrium, and charge neutrality that describe the interdependence of  $Y_p$ ,  $X_{\text{nuc}}$ ,  $\mu_e$ , and  $\tau_{\nu_i}$ .

We prove that the electron degeneracy has important effects indeed, but mainly not in the sense that it suppresses the creation of neutrinos from  $e^-e^+$  pairs and enlarges the electron pressure (Kohri & Mineshige 2002; Kohri et al. 2005). As seen from Figures 4b and 3, the neutrino cooling due to  $e^-e^+$  pair annihilation  $q_{e^-e^+}$  is much smaller than that due to the URCA processes  $q_{\text{URCA}}$ , and the electron pressure is important only in the outer region of the disk where the  $\alpha$ -particle disintegration has not started. Instead, the main effects of electron degeneracy are: (1) It increases  $q_{\text{URCA}}$  greatly, so that the corresponding absorption makes a major contribution to the neutrino optical depth (Fig. 4); (2) It along with the neutronization processes cause  $Y_e$  to become smaller than 0.1 in the inner region of the disk (Fig. 2) where the neutrino cooling is dominant (Fig. 6).

The resulting  $L_{\nu\bar{\nu}}$  is considerably reduced comparing with that in previous works where the electron degeneracy was not considered and  $Y_e$  was taken to be 0.5, however it is still likely to be adequate for GRBs, and its spatial distribution is likely to be anisotropic.

Perhaps the main limitation of our calculations here is that they are one-dimensional. As in most of previous works in the field, we do not study the vertical structure of the disk and instead use the simple 'one-zone' approximation of the vertically-averaged model. In particular, we do not consider the distribution and transport of neutrinos in the vertical direction of the disk, a problem that remains unsolved or even rarely touched (Sawyer 2003). Strictly speaking, a reliable quantitative evaluation of the neutrino annihilation luminosity should require two-dimensional calculations, in which the vertical structure and neutrino transport are self-consistently included. But in view of the fact that most popular models of normal accretion disks (the Shakura-Sunyaev disk model, the slim disk model, and the advection-dominated accretion flow model) are also one-dimensional and have been proved successful, our results here may provide a plausible, though rough, estimate of the luminosity of neutrino-cooled accretion disks.

This work was supported by the National Science Foundation of China under grants 10503003 and 10673009.

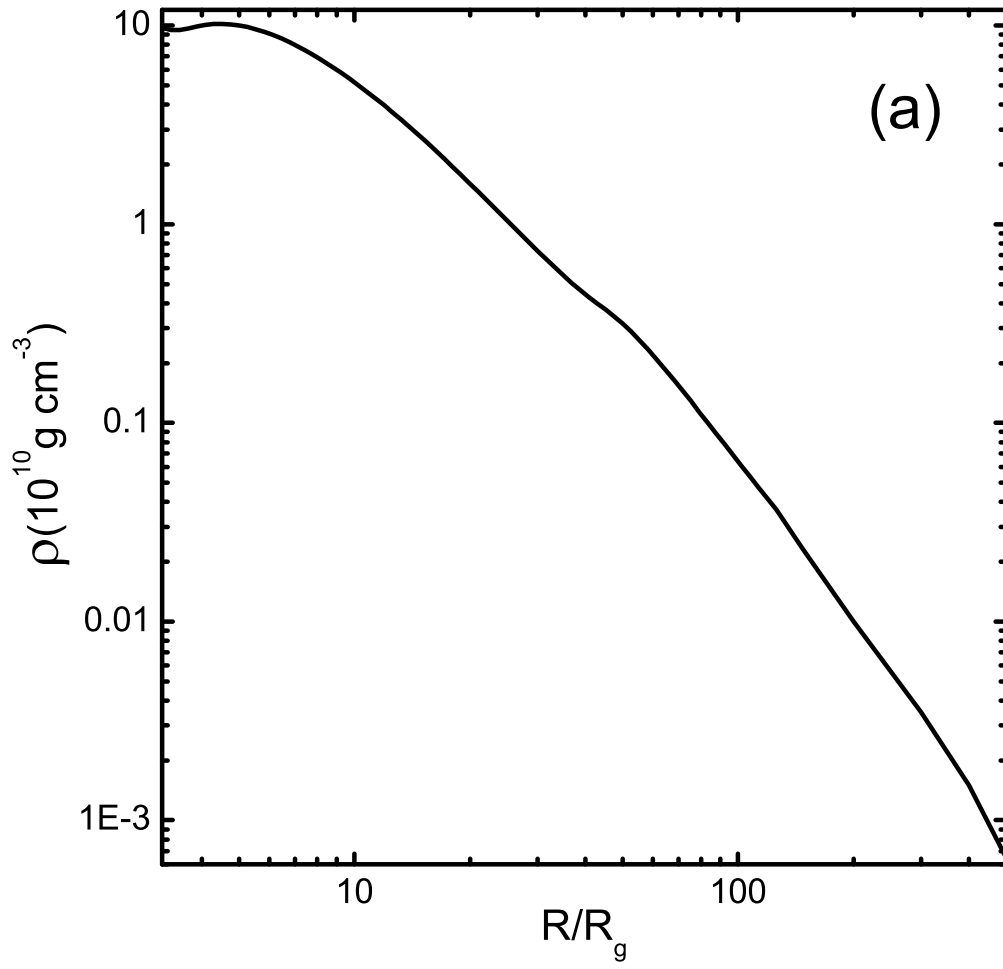
## REFERENCES

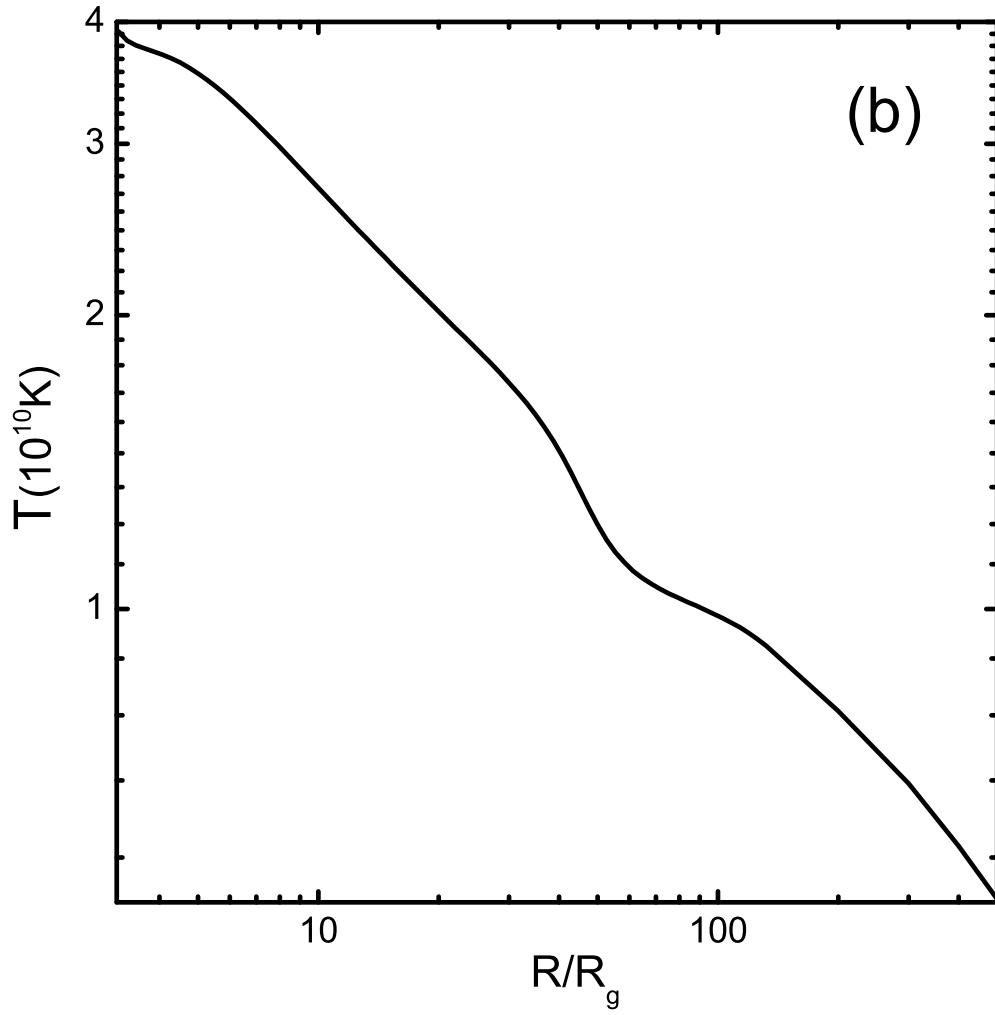
- Beloborodov, A. M. 2003, *ApJ*, 588, 931
- Burrows, A., & Thompson, T. A. 2002, astro-ph/0211404
- Burrows, A., Young, T., Pinto, P., Eastman, R., & Thompson, T. A. 2000, *ApJ*, 539, 865
- Chen, W., & Beloborodov, A. M. 2006, *ApJ*, in press (astro-ph/0607145)
- Di Matteo, T., Perna, R., & Narayan, R. 2002, *ApJ*, 579, 706
- Gu, W.-M., Liu, T., & Lu, J.-F. 2006, *ApJ*, 643, L87
- Hannestad, S., & Raffelt, G. 1998, *ApJ*, 507, 339
- Itoh, N., Adachi, T., Nakagawa, M., Kohyama, Y., & Munakata, H. 1989, *ApJ*, 339, 354  
(erratum 360, 741 [1990])
- Kato, S., Fukue, J., & Mineshige, S. 1998, *Black Hole Accretion Disks* (Kyoto: Kyoto Univ. Press)
- Kohri, K., & Mineshige, S. 2002, *ApJ*, 577, 311
- Kohri K., Narayan, R., & Piran, T. 2005, *ApJ*, 629, 341
- Lee, W. H., Ramirez-Ruiz, E., & Page, D. 2005, *ApJ*, 632, 421
- Mészáros, P. 2002, *ARA&A*, 40, 137
- Meyer, B. S. 1994, *ARA&A*, 32, 153
- Paczyński, B. & Wiita, P. J. 1980, *A&A*, 88, 23
- Popham, R., & Narayan, R. 1995, *ApJ*, 442, 337
- Popham, R., Woosley, S. E., & Fryer, C. 1999, *ApJ*, 518, 356
- Rosswog, S., Ramirez-Ruiz, E., & Davies, M. B. 2003, *MNRAS*, 345, 1077
- Ruffert, M., Janka, H.-T., & Schäfer, G. 1996, *A&A*, 311, 532
- Ruffert, M., Janka, H.-T., Takahashi, K., & Schäfer, G. 1997, *A&A*, 319, 122
- Sawyer, R. F. 2003, *Phys. Rev. D*, 68, 063001

Shapiro, S. L., & Teukolsky, S. L. 1983, *Black Holes, White Dwarfs and Neutron Stars*(New York: Wiley)

Yuan, Y.-F. 2005, *Phys. Rev. D*, 72, 013007

Zhang, B., & Mészáros, P. 2004, *Int. J. Mod. Phys. A*, 19, 2385





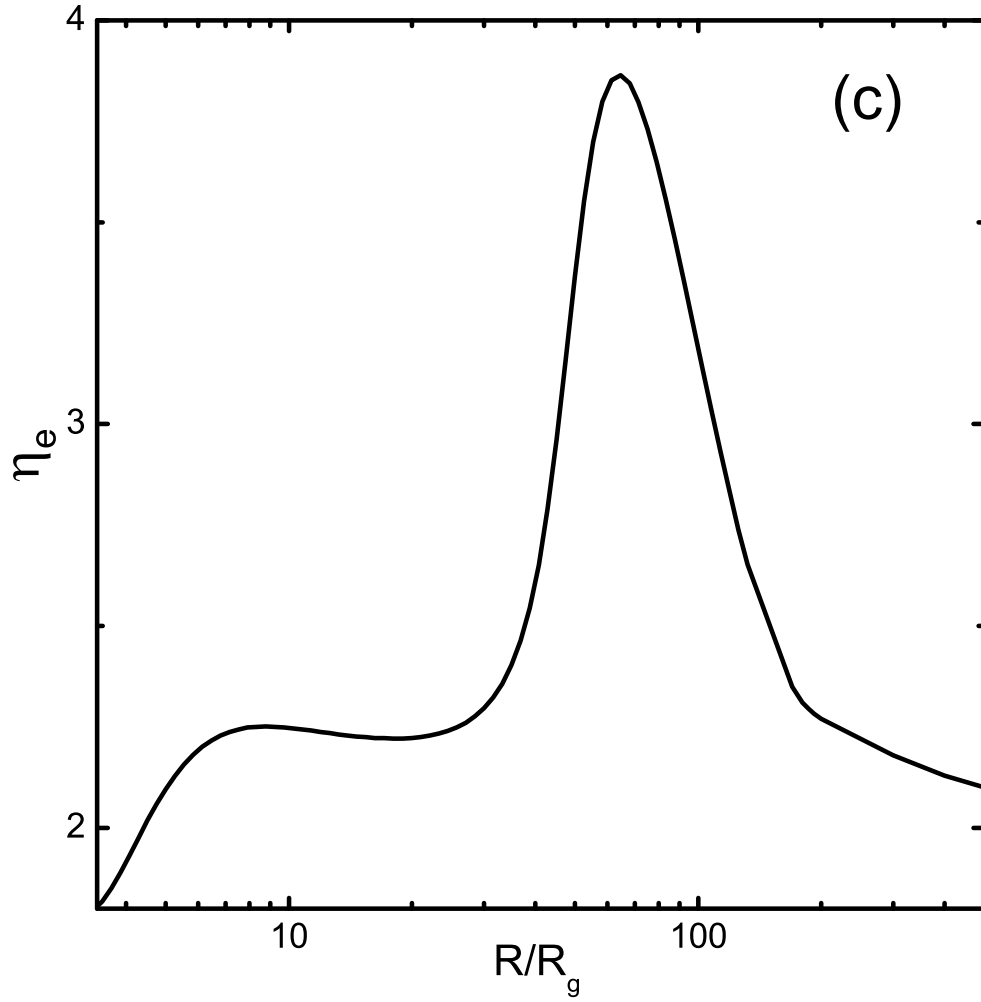


Fig. 1.— (a) Density  $\rho$ , (b) Temperature  $T$ , and (c) electron degeneracy  $\eta_e$  as functions of radius  $R$ , with the black hole mass  $M = 3M_\odot$ , mass accretion rate  $\dot{M} = 1M_\odot \text{ s}^{-1}$ , viscosity parameter  $\alpha = 0.1$ , and the accreted specific angular momentum  $j = 1.8cR_g$ .

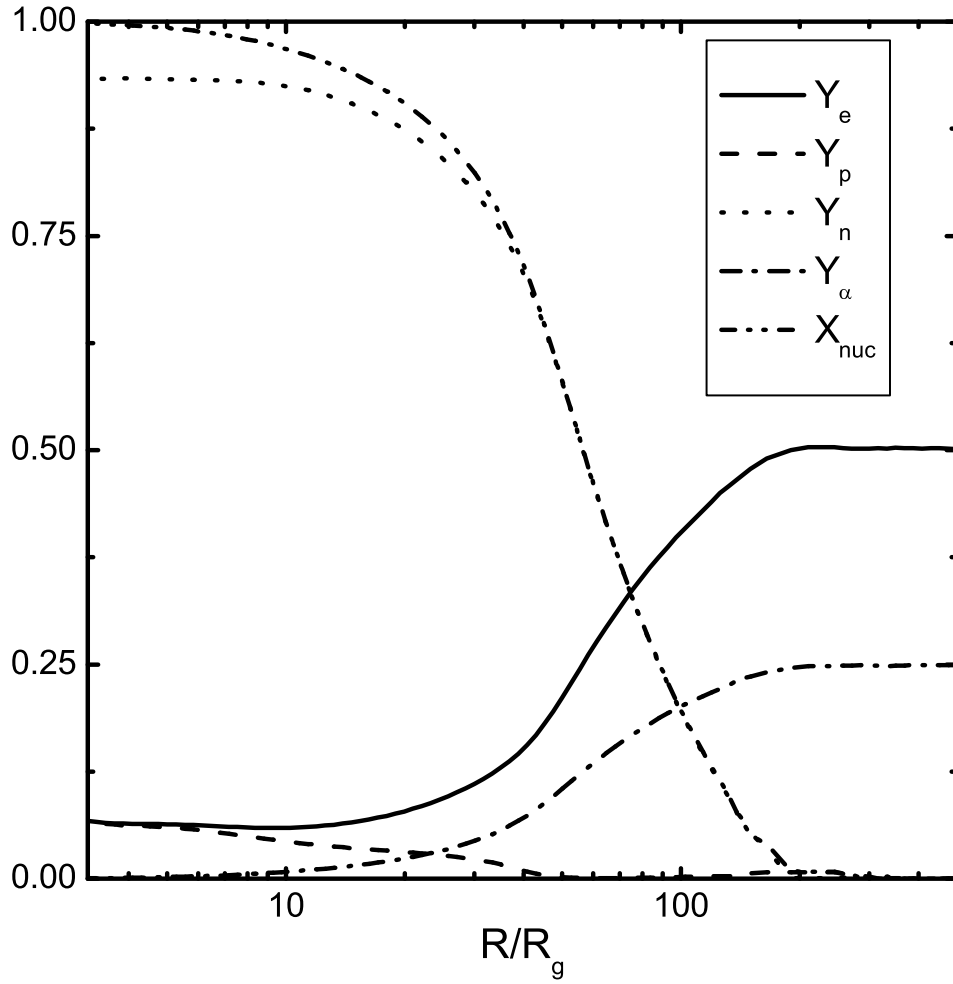


Fig. 2.— Electron fraction  $Y_e$ , free proton fraction  $Y_p$ , free neutron fraction  $Y_n$ ,  $\alpha$ -particle fraction  $Y_\alpha$ , and free nucleon fraction  $X_{\text{nuc}}$  as functions of  $R$ , with the same constant parameters as in Fig. 1.

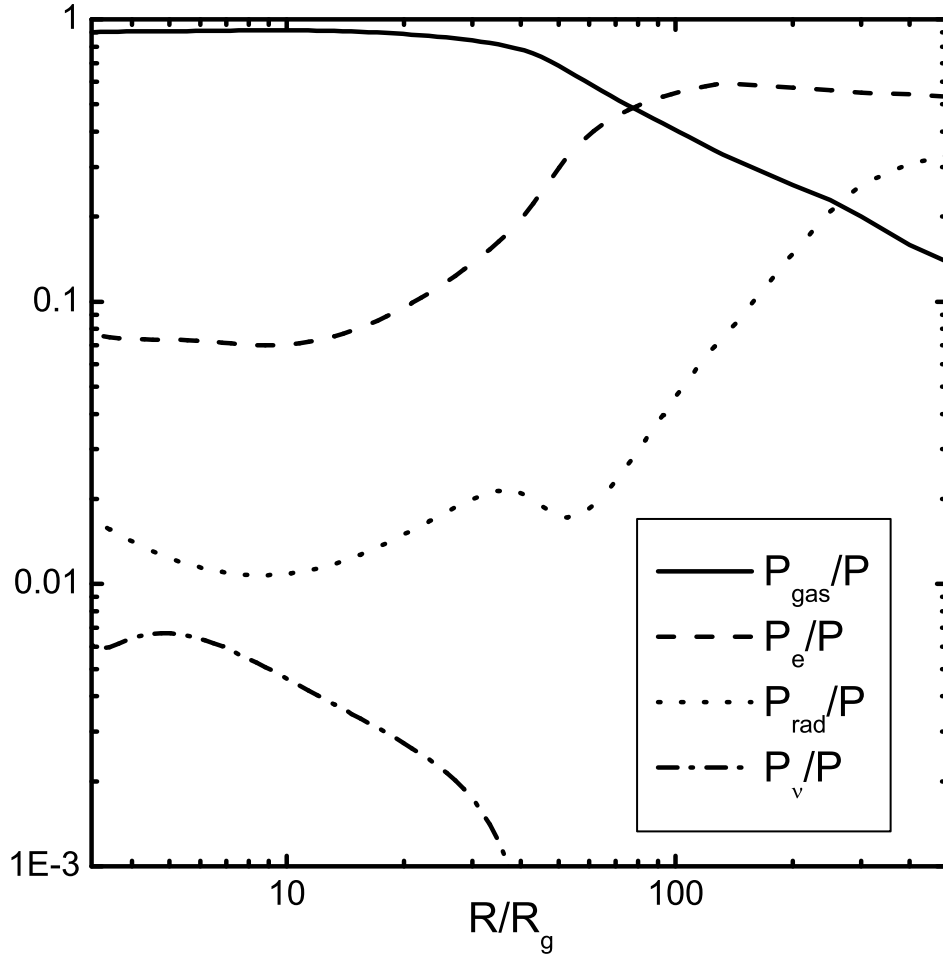
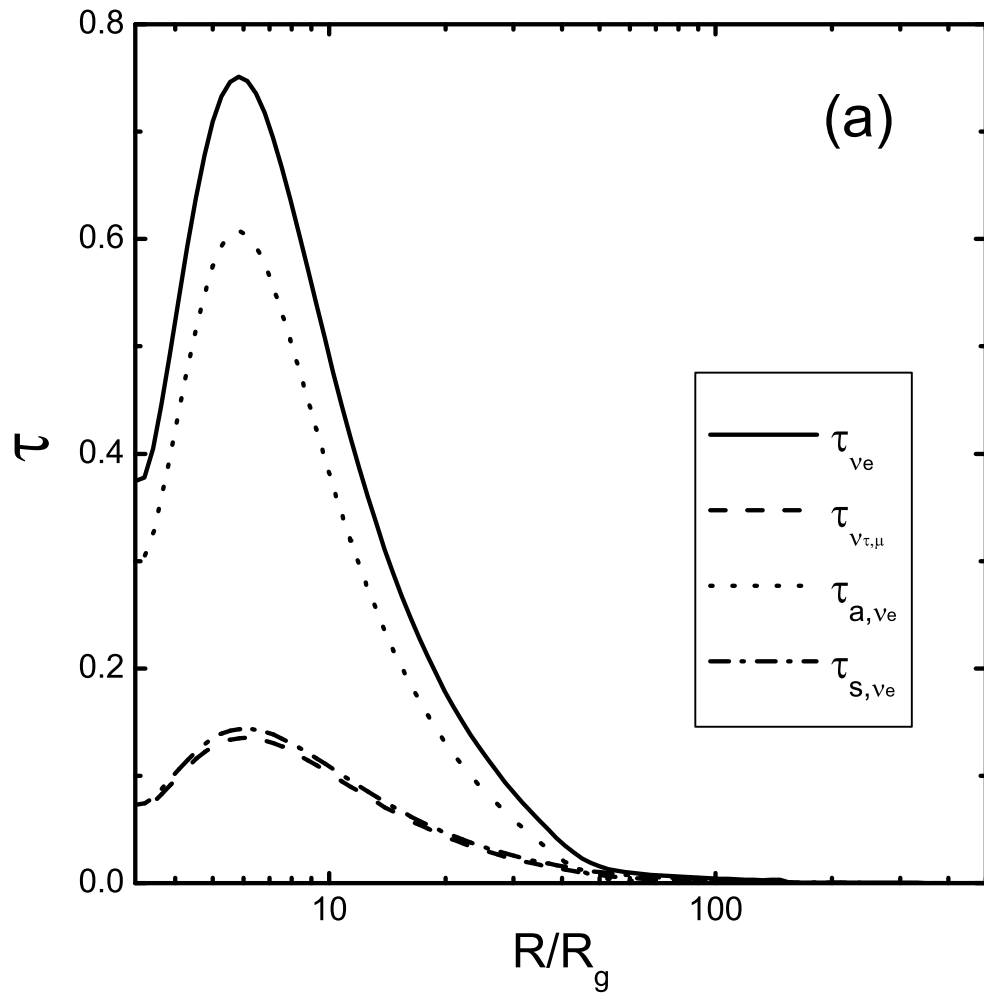
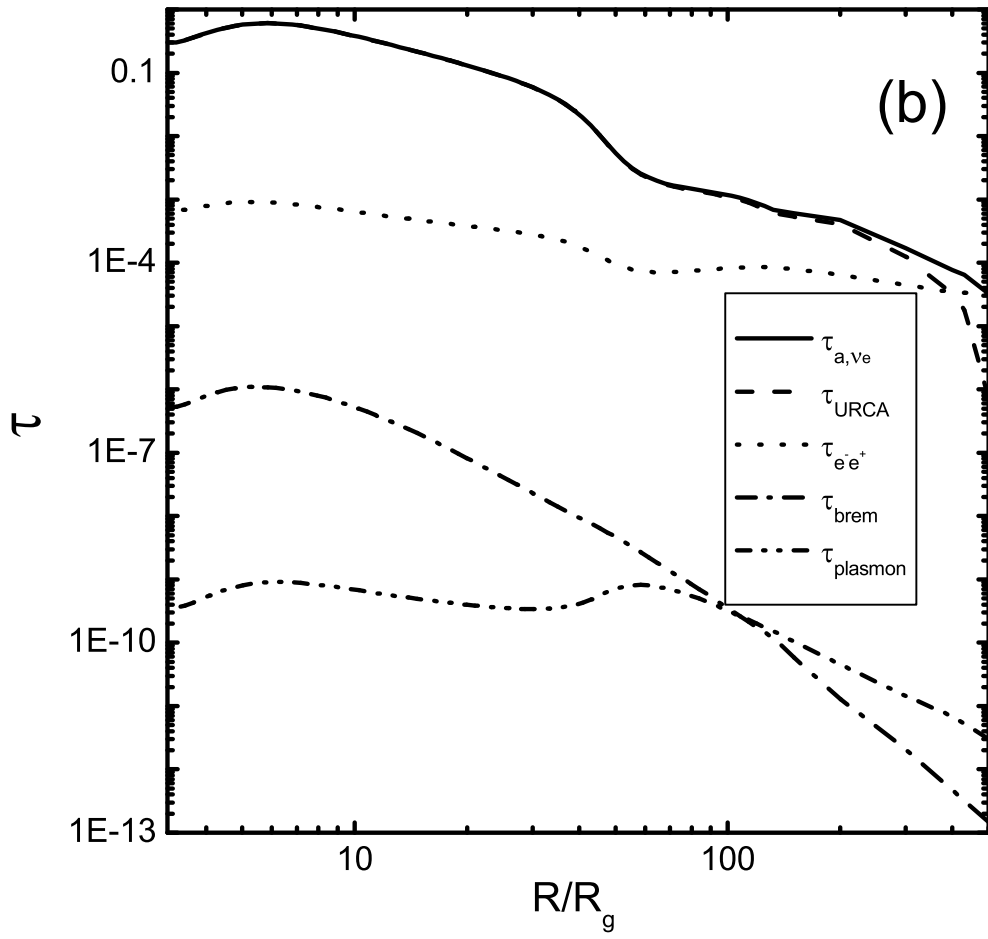


Fig. 3.— Contributions to the total pressure  $P$  from free nucleons and  $\alpha$ -particles  $P_{\text{gas}}$ , from degenerate electrons  $P_e$ , from photon radiation  $P_{\text{rad}}$ , and from neutrinos  $P_\nu$ , as functions of  $R$ , with the same constant parameters as in Fig. 1.





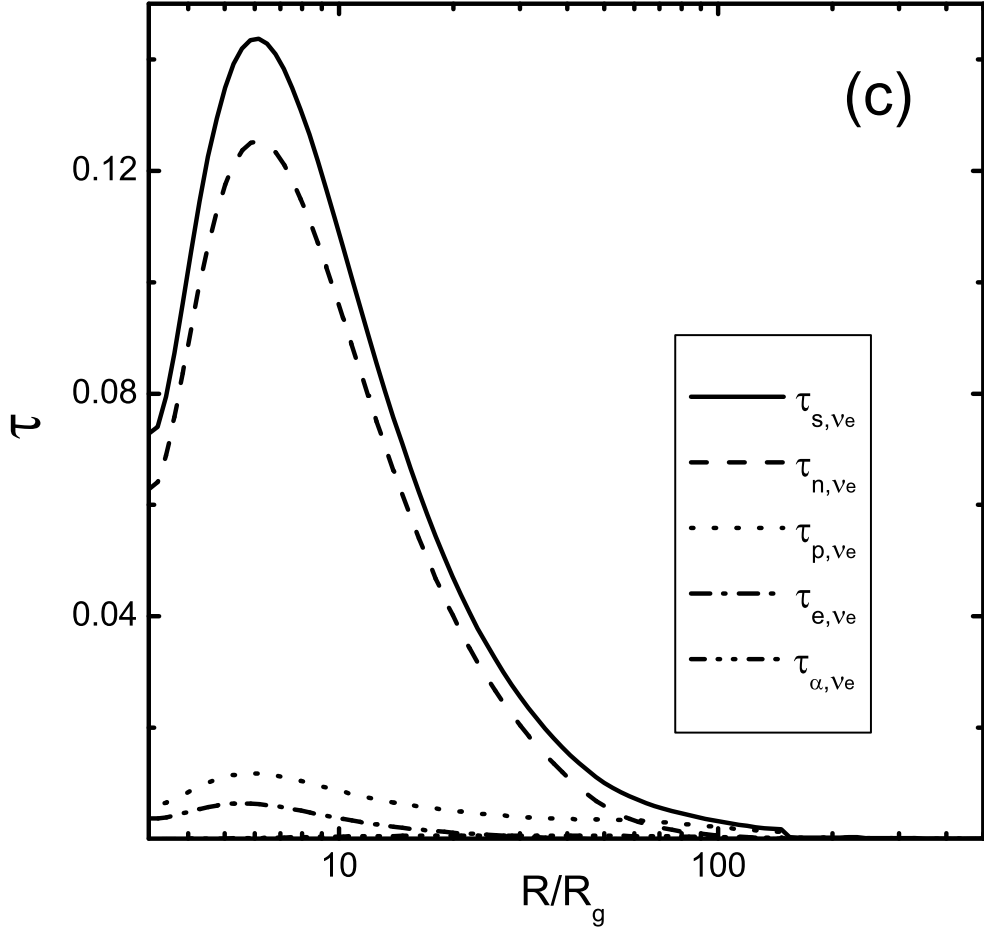


Fig. 4.— (a) Total optical depth for electron neutrinos  $\tau_{\nu_e}$ , total optical depth for  $\tau$ -neutrinos and  $\mu$ -neutrinos  $\tau_{\nu_{\tau, \mu}}$ , absorption optical depth for electron neutrinos  $\tau_{a, \nu_e}$ , and scattering optical depth for electron neutrinos  $\tau_{s, \nu_e}$ ; (b) Quantity  $\tau_{a, \nu_e}$  and its contributions from the URCA processes  $\tau_{\text{URCA}}$ , from neutrino annihilation  $\tau_{e^-e^+}$ , from nucleon-nucleon bremsstrahlung  $\tau_{\text{brem}}$ , and from the inverse process of plasmon decay  $\tau_{\text{plasmon}}$ ; and (c) Quantity  $\tau_{s, \nu_e}$  and its contributions due to free neutrons  $\tau_{n, \nu_e}$ , due to free protons  $\tau_{p, \nu_e}$ , due to electrons  $\tau_{e, \nu_e}$ , and due to  $\alpha$ -particles  $\tau_{\alpha, \nu_e}$  as functions of  $R$ , with the same constant parameters as in Fig. 1.

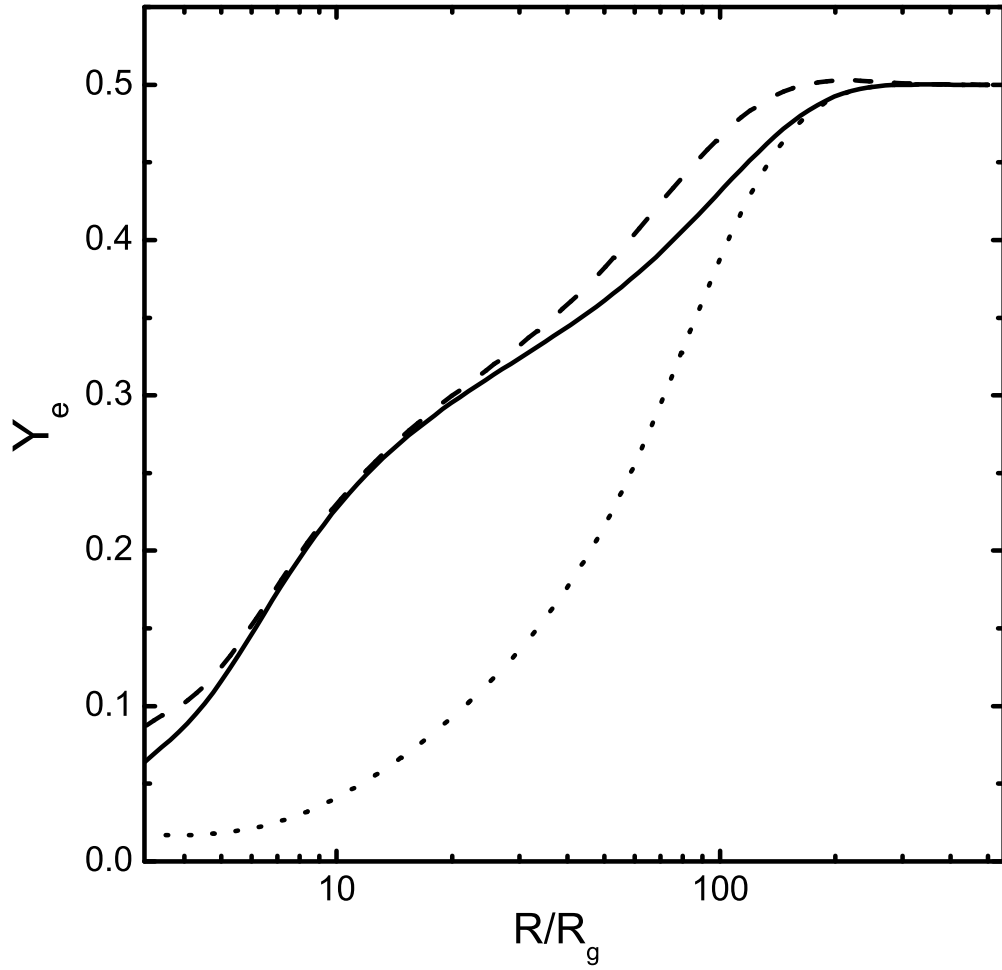


Fig. 5.— Solid, dashed, and dotted lines draw  $Y_e$  calculated with equations (42), (46), and (47), respectively, with the same constant parameters as in Fig. 1 except for  $\dot{M} = 5M_\odot \text{ s}^{-1}$ .

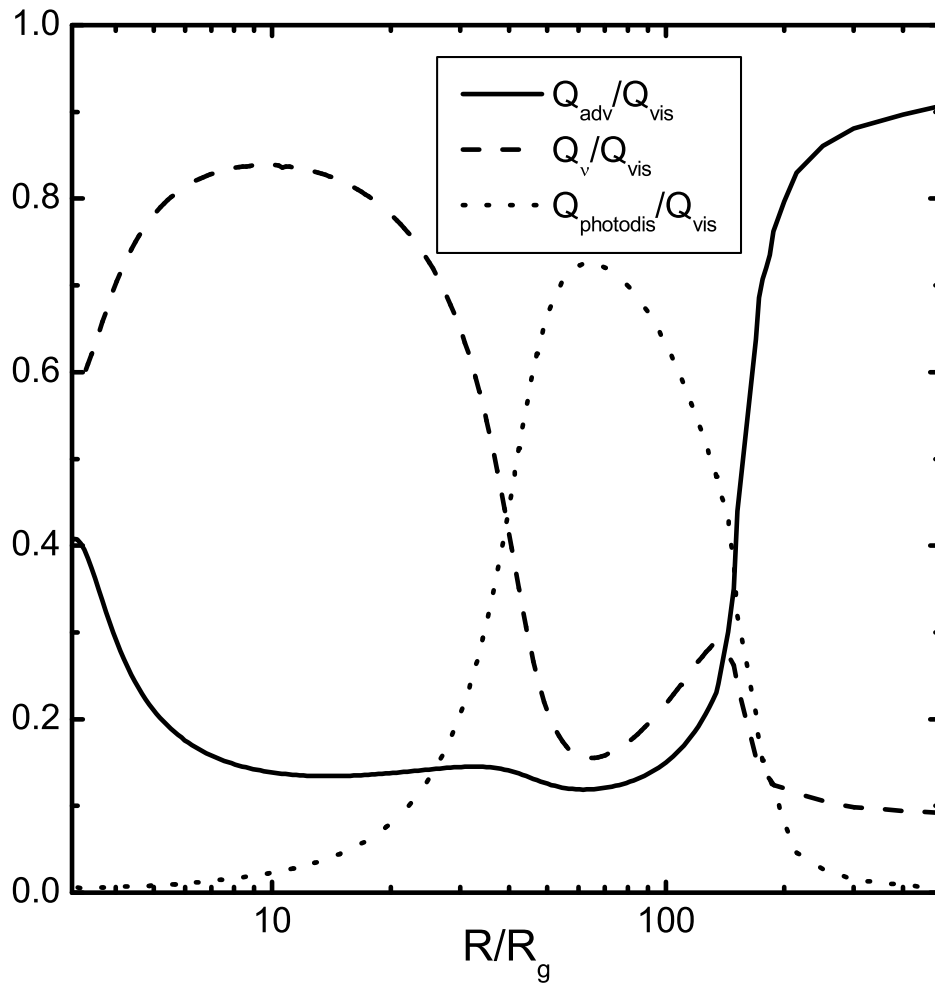


Fig. 6.— Ratios of the advective cooling rate  $Q_{\text{adv}}$ ,  $\alpha$ -particle photodisintegration cooling rate  $Q_{\text{photodis}}$ , and neutrino cooling rate  $Q_{\nu}$  to viscous heating rate  $Q_{\text{vis}}$  as functions of  $R$ , with the same constant parameters as in Fig. 1.

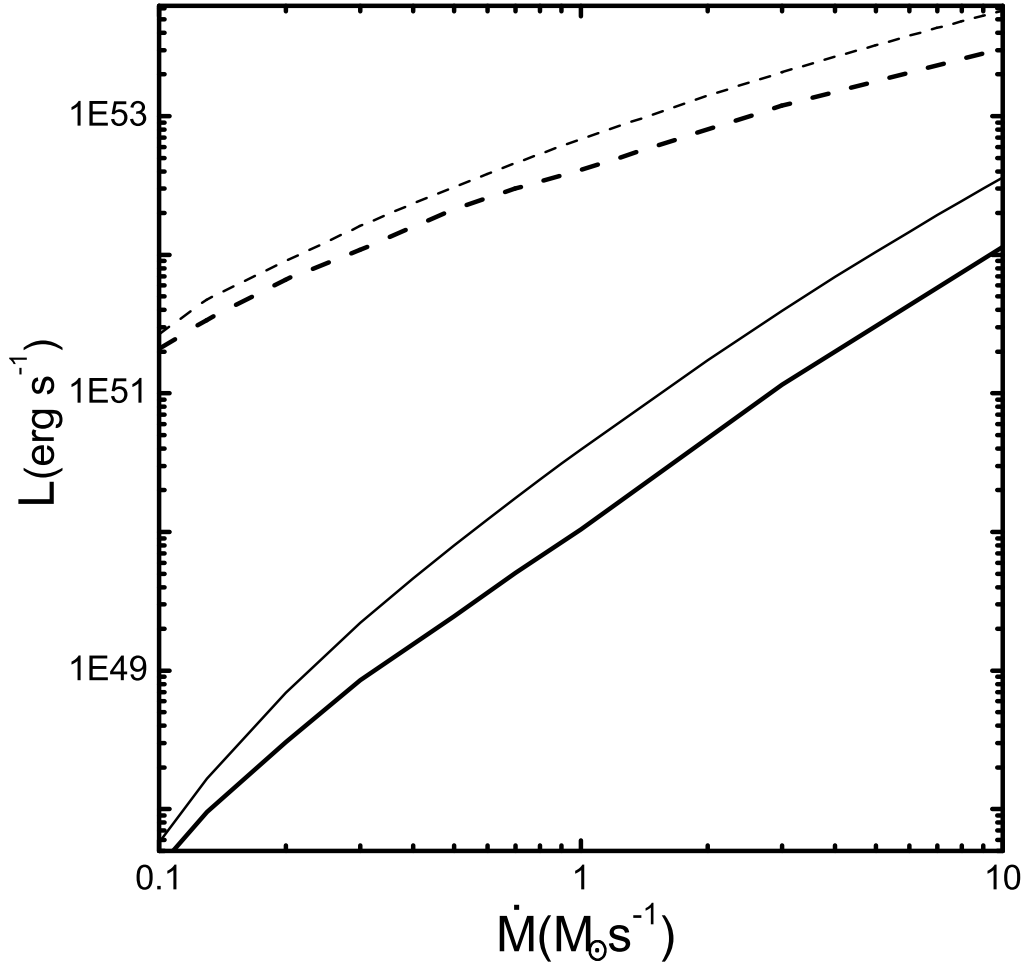


Fig. 7.— Neutrino radiation luminosity  $L_{\nu}$  (the thick dashed line) and neutrino annihilation luminosity  $L_{\nu\bar{\nu}}$  (the thick solid line) for varying  $\dot{M}$ . The overestimated  $L_{\nu}$  (the thin dashed line) and  $L_{\nu\bar{\nu}}$  (the thin solid line) taken from Gu et al. (2006) are also given. The constant parameters  $M$ ,  $\alpha$ , and  $j$  are the same as in Fig. 1.

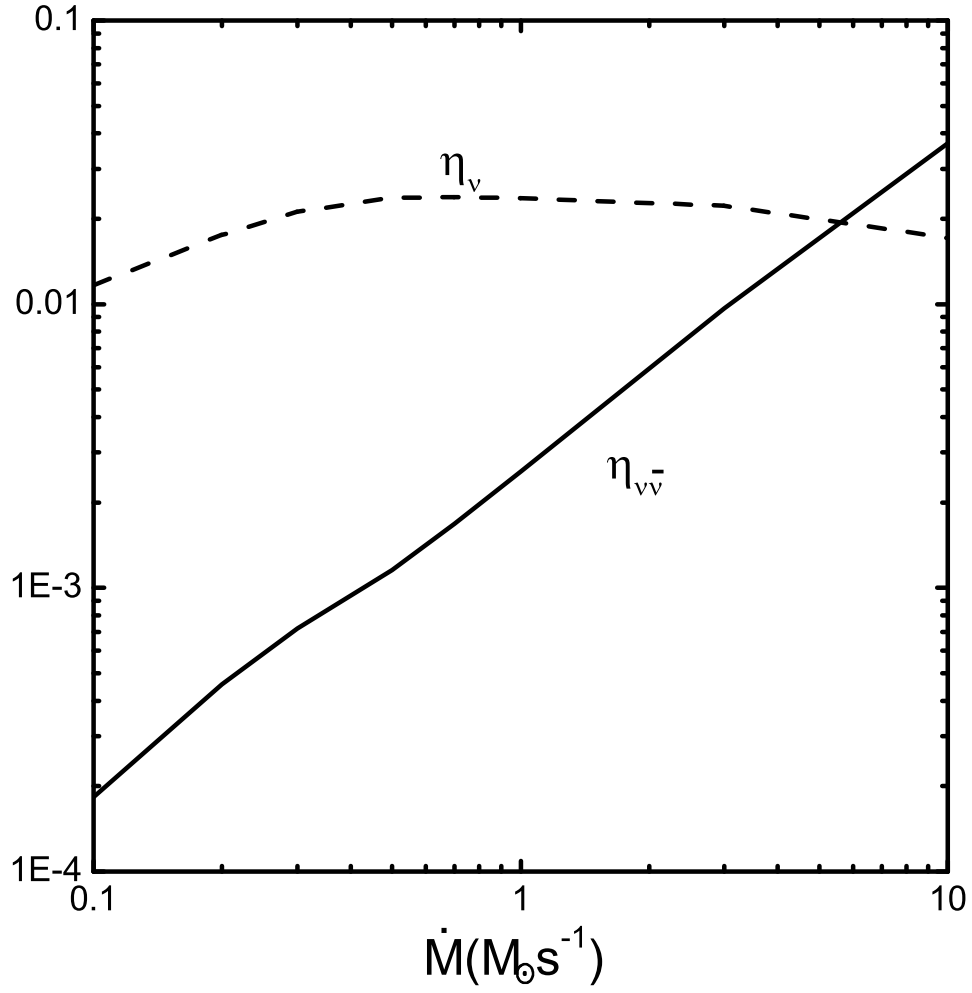


Fig. 8.— Neutrino radiation efficiency  $\eta_{\nu}$  and neutrino annihilation efficiency  $\eta_{\nu\bar{\nu}}$  for varying  $\dot{M}$ , with the same  $M$ ,  $\alpha$ , and  $j$  as in Fig. 1.

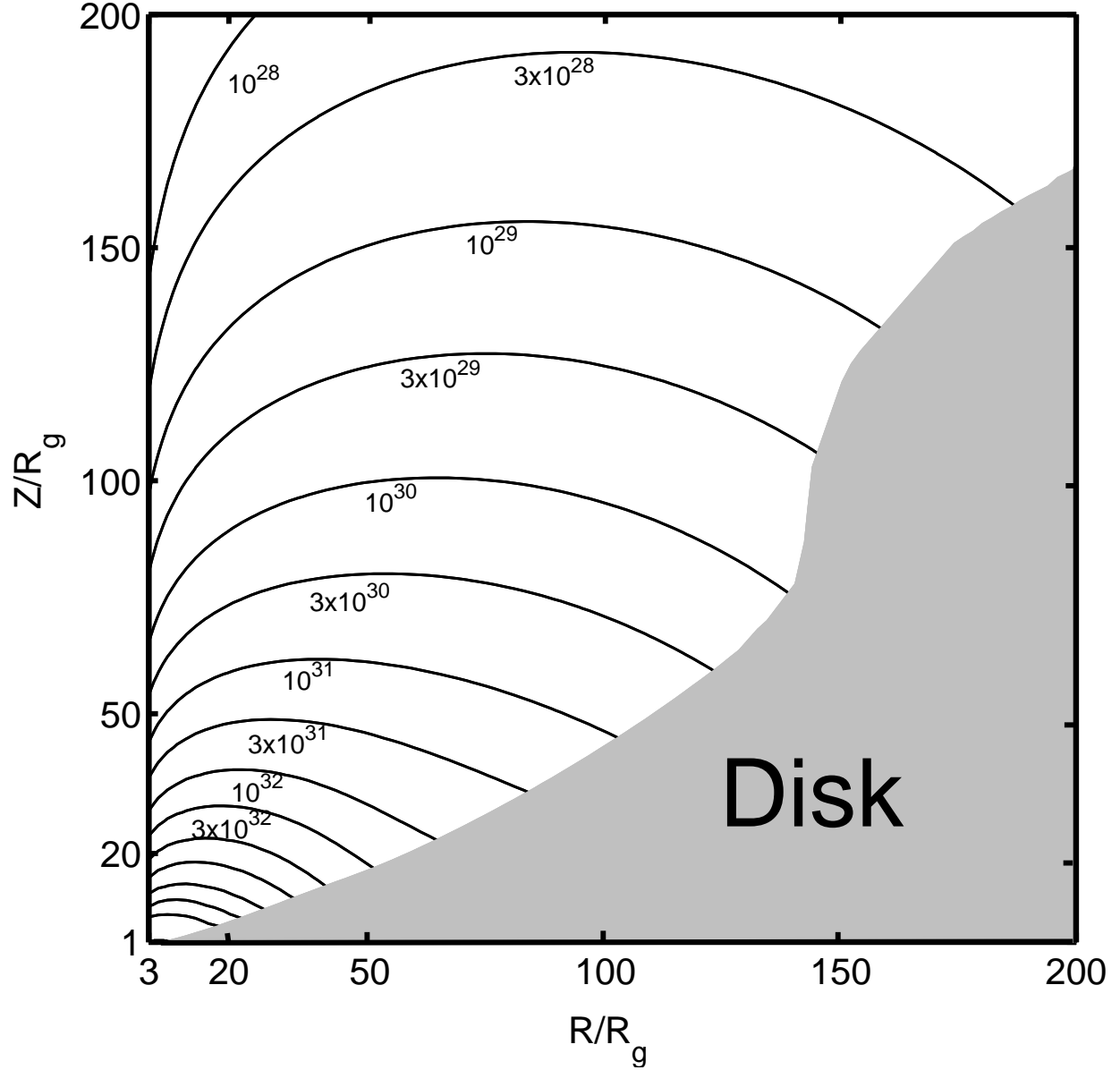


Fig. 9.— Contours of the neutrino annihilation luminosity of a circle with cylindrical coordinates  $R$  and  $Z$ . The number attaching to each line is this luminosity in units of ( $\text{erg s}^{-1} \text{cm}^{-2}$ ). The shaded region shows the accretion disk. The constant parameters are the same as in Fig. 1.